12-1-2018

A New Normal for Streamflow in California in a Warming Climate: Wetter Wet Seasons and Drier Dry Seasons

Iman Mallakpour
University of California

Mojtaba Sadegh
Boise State University

Amir AghaKouchak
University of California

Publication Information

Mallakpour, Iman; Sadegh, Mojtaba; and AghAkouchak, Amir. (2018). "A New Normal for Streamflow in California in a Warming Climate: Wetter Wet Seasons and Drier Dry Seasons". *Journal of Hydrology, 567*, 203-211. doi: http://dx.doi.org/10.1016/j.jhydrol.2018.10.023

A New Normal for Streamflow in California in a Warming Climate: Wetter Wet Seasons and Drier Dry Seasons

IMAN MALLAKPOUR[1], MOJTABA SADEGH[2], AMIR AGHAKOUCHAK[1]

[1] Department of Civil and Environmental Engineering, University of California, Irvine, CA 92697, USA

[2] Department of Civil Engineering, Boise State University, Boise, ID

Manuscript submitted to

Journal of Hydrology

Corresponding author address: Amir AghaKouchak (amir.a@uci.edu)

Abstract

In this study, we investigate changes in future streamflows in California using bias-corrected and routed streamflows derived from global climate model (GCM) simulations under two representative concentration pathways (RCPs): RCP4.5 and RCP8.5. Unlike previous studies that have focused mainly on the mean streamflow, annual maxima or seasonality, we focus on projected changes across the distribution of streamflow and the underlying causes. We report opposing trends in the two tails of the future streamflow simulations: lower low flows and higher high flows with no change in the overall mean of future flows relative to the historical baseline (statistically significant at 0.05 level). Furthermore, results show that streamflow is projected to increase during most of the rainy season (December to March) while it is expected to decrease in the rest of the year (i.e., wetter rainy seasons, and drier dry seasons). We argue that the projected changes to streamflow in California are driven by the expected changes to snow patterns and precipitation extremes in a warming climate. Changes to future low flows and extreme high flows can have significant implications for water resource planning, drought management, and infrastructure design and risk assessment.

1. Introduction

Excessive deviation from the normal hydrological condition in river systems can impose catastrophic socioeconomic impacts (e.g., fatalities, infrastructure and property damage, agricultural loss, and disruption of daily life) and challenge the existing water management plans (e.g., Demaria et al., 2016; Nazemi & Wheater, 2014). Current methods for design of hydraulic structures (e.g., dams, bridges, levees, spillways, culverts) are based on the so-called stationary assumption that assumes the statistics of extremes and distribution of the underlying variables do not change over time (Sadegh et al., 2015). The stationarity assumption requires that the distribution of past observed events and the statistics of observed extremes are a good representative of possible future conditions (e.g., Koutsoyiannis, 2006; Read & Vogel, 2015; Villarini et al., 2009). However, in recent years, studies have shown that different natural and anthropogenic factors (e.g., land use land cover, climate, urbanization, watershed modification) can alter streamflow characteristics (Alfieri et al., 2015; Beighley et al., 2003; Hailegeorgis & Alfredsen, 2017; Krakauer & Fung, 2008; Luke et al., 2017; Mallakpour et al., 2017; Mallakpour & Villarini, 2015; Villarini et al., 2015), thus questioning the validity of the stationary assumption (Cheng et al., 2014).

The projected warming and expected changes in precipitation and snow patterns are anticipated to change river flows (e.g., Alfieri et al., 2015; McCabe & Wolock, 2014; Nazemi & Wheater, 2014). A warmer climate is expected to intensify the hydrological cycle, increasing the frequency and/or intensity of extreme events such as droughts and floods (e.g., Das et al., 2013; Milly et al., 2005; Pachauri et al., 2015; Voss et al., 2002; Wang et al., 2017). Warmer land surface and water bodies may increase evaporation (Scheff & Frierson, 2014), and enlarge atmospheric moisture holding capacity (the Clausius–Clapeyron relation; O'Gorman & Muller, 2010); both of which can contribute to the changes in river flows (e.g., Alfieri et al., 2015).

Moreover, a warmer climate may drive earlier snowmelt, decline in snowpack, change in seasonality of river flows and changes in snow to rain ratio (e.g., Cayan et al., 2001; Harpold et al., 2017; Knowles et al., 2006; Mao et al., 2015; Neelin et al., 2013; Stewart et al., 2005). These changes are even more important in regions like California, where streamflow relies on winter snow accumulation (e.g., Diffenbaugh et al., 2015; Li et al., 2017). Several studies have documented that warm and wet storms brought by atmospheric rivers (AR) during winter may cause severe flooding in California (e.g., Barth et al., 2016; Dettinger, 2011; Leung & Qian, 2009; Ralph et al., 2013). *Jeon et al. (2015)* used 10 CMIP5 climate models to show that AR events in warming climate would bring more frequent and severe storms to California in the future. Similarly, *Payne and Magnusdottir (2015)* used 28 CMIP5 models in a study where they projected up to 35% increase in AR landfall days. *Dettinger (2011)* have shown that potential increases in the magnitude and frequency of AR events in the future can cause more severe and frequent flooding events in California.

In recent years, California has experienced a series of flooding events (Vahedifard et al., 2017) on the heels of a 5-year drought (e.g., AghaKouchak et al., 2014; Hardin et al., 2017; Shukla et al., 2015). In 2017, a major flood in Northern California led to structural failure of Oroville Dam's spillway that triggered the evacuation of about 200,000 people. In another event, a levee breach near Manteca, CA, provoked the local government to evacuate about 500 people (Vahedifard et al., 2017). In light of the occurrence of recent extreme events over Northern California, this study aims to answer a simple but important question: how will streamflow distribution change for Northern California under a warming climate? The insights gained by improving our understanding of the possible changes in the direction and magnitude of streamflow can have profound implications on adaptation strategies to cope with the future extreme events (i.e., floods and droughts) and better managing of the water resources (*Villarini et al. (2015))*.

Several studies have previously investigated projected changes in the hydrologic cycle over California from different perspectives (AghaKouchak et al., 2014; Ashfaq et al., 2013; Burke & Ficklin, 2017; Diffenbaugh et al., 2015; Hailegeorgis & Alfredsen, 2017; Li et al., 2017; Thorne et al., 2015; Zhu et al., 2005). Our current state of the knowledge is mostly limited to possible changes in average annual, annual maxima or seasonal streamflow mainly using gridded runoff products. While most studies reported changes in seasonality of streamflow over California, there is no consensus on the direction (sign) of change in the flow regime. Some studies projected little or no change in future annual streamflow over California (e.g., Regonda et al., 2005; Stewart et al., 2005; Thorne et al., 2015), while others projected a decreasing trend in streamflow (e.g., Berghuijs et al., 2014; Das, et al., 2011b; Li et al., 2017). Furthermore, there are a number of studies that have focused only on the peak flows, where they projected increases in the magnitude of flooding in California under climate change scenarios (e.g., Das et al., 2011a, 2013; M. D. Dettinger & Ingram, 2012). The aim of the current study is to get a more comprehensive view of possible changes in streamflow distribution over Northern California by analyzing the possible changes in different streamflow quantiles. Unlike previous studies, and instead of gridded runoff simulations, we employed a unique data set generated for the 4th California Climate Assessment group, which includes climate model simulations, bias corrected, and routed for 59 sites across Northern California for the period of 1950–2099. Moreover, in order to investigate the direction of change in river discharge, in addition to investigating the mean flows, we examine changes over different parts of the discharge regime (from low to high flows).

2. Data and Method

Daily streamflow (m^3/s) data for 59 locations across Northern California were developed at the Scripps Institution of Oceanography, University of California San Diego and acquired from the 4th California Climate Assessment group (Pierce et al., 2014, 2015; Figure S1). The Variable Infiltration Capacity (VIC) land surface model (Lohmann et al., 1996, 1998), a macro-scale hydrological model framework that simulates surface and subsurface processes, was forced with downscaled global climate model (GCM) simulations to route streamflow at a daily temporal scale. The use of downscaling techniques to convert the coarse spatial resolution in the GCMs to high resolution hydrological variables is an inevitable step for the climate change impacts assessment studies (Mehrotra & Sharma, 2015). The VIC model is driven by the high-resolution Localized Constructed Analogs (LOCA) downscaled and bias-corrected minimum and maximum temperature, and precipitation. The LOCA method calculates the simulated hydrological variable (with a grid resolution of 0.0625°) by using a multiscale spatial matching framework in order to pick suitable analog days from historical observations. Pierce et al., 2014 mentioned that the motivation behind developing the LOCA method was to have a framework that can better preserve regional patterns in temperature and precipitation, and also better represent the maximum temperature and precipitation for California. There are a number of limitations associated with the use of any downscaling technique including simplification of the physical processes that may result in systematic errors that can be distributed between temperature and precipitation (Mehrotra & Sharma, 2012, 2016). More detailed description of the downscaling and bias-correction methods to develop the streamflow dataset we used here, together with limitations and advantages, can be found in Pierce et al., 2014, 2015.

The VIC model parameters were obtained from the University of Colorado hydrologically based dataset for entire California (Livneh et al., 2013; Maurer et al., 2002). The details on the VIC model, together with strengths, weakness and parameterization of it can be found in the *Pierce et al. (2016)*. As Pierce et al. (2016) indicated while the VIC hydrological modeling framework is widely used in the hydrological community, the use of any hydrological model will result in some degree of uncertainty to projected climate variables and future studies are encouraged to perform similar analysis using additional land surface models. Furthermore, it is noteworthy that the antecedent moisture conditions in a drying climate were merely accounted for by the energy balance scheme of the VIC model, and further uncertainty analysis is required to scrutinize such impacts on the trends of streamflow. This will be the subject of a future study.

In this study, the bias-corrected inputs to the VIC model are based on ten GCMs from the Fifth Coupled Model Intercomparison Project (CMIP5; Table S1) and two representative concentration pathways (RCPs): RCP4.5 and RCP8.5. We use these ten models, selected from 32 different GCMs by the Climate Action Team Research Working Group of the 4th California's Climate Change Assessment, as they cover a wide range of possible conditions that California may confront in the future (CDWR, 2015). Furthermore, the future climate related policies and actions in California would be based on the outputs of these climate models that is provided by the 4th California's Climate Change Assessments (**www.ClimateAssessment.ca.gov**).

For each site and scenario, we calculated the ensemble median of daily streamflow based on all the ten climate models from 1950 to 2099 using 1950 to 2005 as the historical baseline period and 2020 to 2099 as the projection period. To investigate changes in the magnitude and direction of discharge, we computed annual time series for different discharge quantiles (from low to high flows) of the daily streamflow for each of the 59 locations (Lins & Slack, 1999; Villarini & Strong, 2014). We then use the nonparametric Mann-Kendall test (Kendall & Gibbons, 1990; Mann, 1945) to detect monotonic trends in different parts of the streamflow distribution. An extensive discussion on the Mann-Kendall test can be found in *Helsel & Hirsch (1992).* The test evaluates the null hypothesis (H_0) of no statistically significant change against the alternative hypothesis (H_a) of a statistically significant trend in the time series at 0.05 significance (95% confidence) level. We also examined the projected change in the magnitude and direction of river discharge based on two hydrological indices, namely 7-day peak flow and 7-day low flow (see Supplementary Material Section S1; Monk et al., 2007; Olden & Poff, 2003; Richter et al., 1996, 1998). Finally, we used the projected change in the mean monthly flows to compare the streamflows over the wet seasons versus the warm seasons to get insight about the possible seasonal changes in streamflow. We compared the mean of the hydrological indices in the projection period relative to the baseline period under the RCP 4.5 and 8.5 by computing normalized percent change: ($\frac{Future - Historical}{Historical} \times 100$).

3. Results

Figure 1 shows presence/absence of statistically significant trends, at 5% level, in the annual mean (panel A-C), annual minima (panel D-F) and annual maxima (panel G-I) of ensemble median of daily streamflow data. Overall, out of the 59 locations, none exhibits statistically significant changes in the annual mean of daily streamflow for both the historical forcing (figure 1A) and the RCP 4.5 scenario (figure 1B). Similar behavior is observed for the RCP8.5 scenario, with only 2 locations showing statistically significant changes in the annual mean of streamflow (Figure 1C). Lack of pronounced signal of change in the annual mean discharge is also observed when we explore trends in the annual volume of ensemble daily streamflow data (Figure S2). These results are consistent with previous studies revealing that future annual mean flow and annual volume of water are not projected to change significantly relative to the baseline (e.g., Regonda et al., 2005; Stewart et al., 2005; Thorne et al., 2015).

However, trends and patterns fundamentally change when investigating the upper and lower tails of the streamflow distribution. Figures 1D-E show the changes in the magnitude of annual minima. Although the signal of change is relatively weak for the historical period (Figure 1 E; only 8 out of 59 sites show statistically significant change), it becomes much stronger when we explore changes in the projection period. As shown, 19 and 54 sites (out of 59) exhibit statistically significant decreasing trends in the discharge annual minima under the RCP 4.5 (Figure 1E) and 8.5 (Figure 1F) scenarios, respectively. Investigating annual maxima reveals opposing trends: 27 sites show statistically significant increasing trends in the baseline period, whereas 29 and 55 sites exhibit statistically significant increasing trends under the RCP 4.5 (Figure 1H) and RCP 8.5 (Figure 1I) scenarios, respectively. Therefore, climate models point to a widespread decreasing (increasing) trends in the annual minima (maxima) over Northern California. Under the RCP 8.5 scenario changes in the annual minimum and maximum discharge are larger and widespread over the entire Northern California.

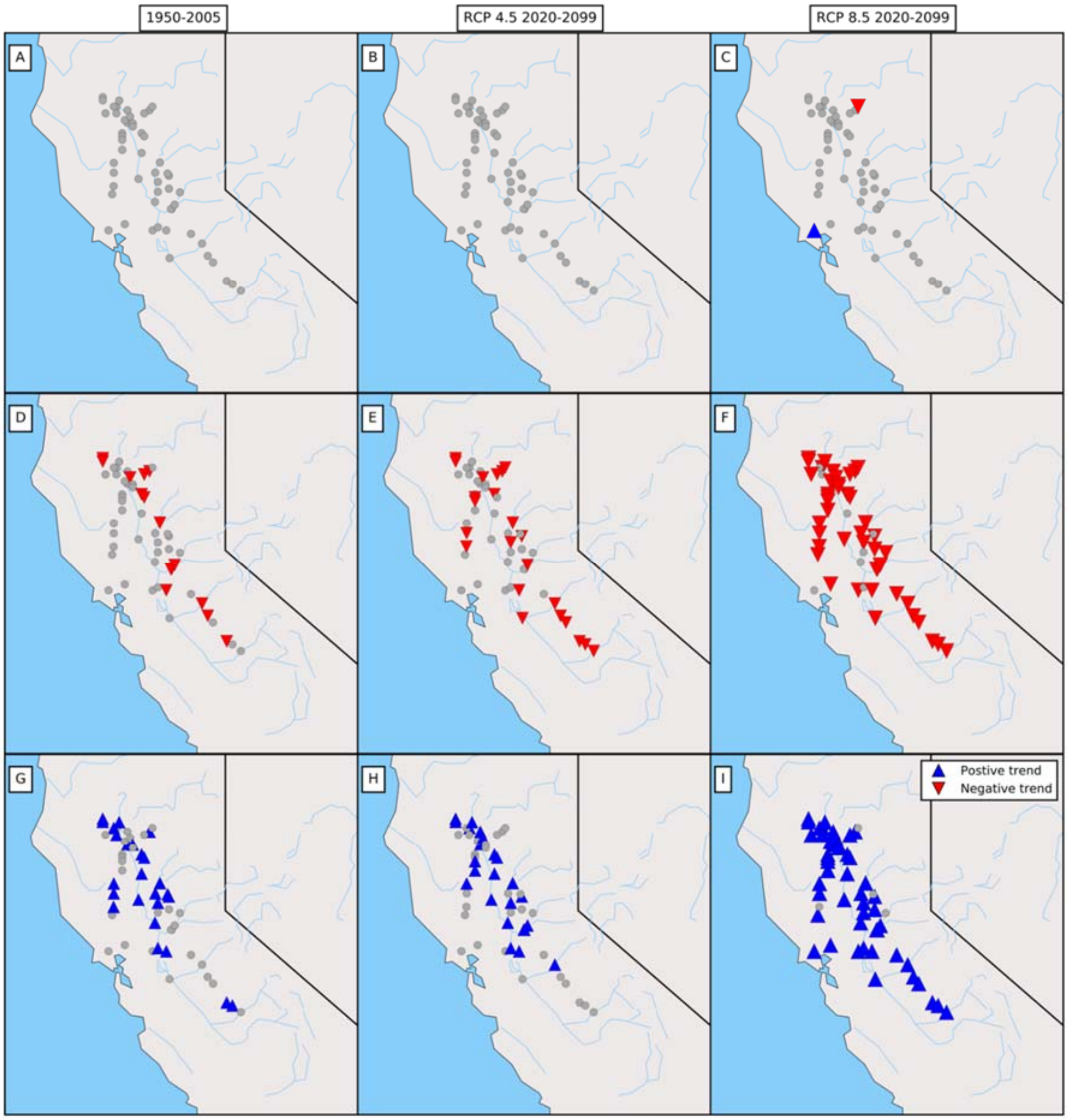

Figure 1: Statistically significant trends in the annual mean (panel A-C), annual minima (panel D-F) and annual maxima (panel G-I) flows over Northern California. Left panels summarize the results for the historical baseline period. Middle and right panels represent change in the projection period under the RCP 4.5 and 8.5 scenarios, respectively. Positive and negative trends are presented with upward blue, and downward red triangles, respectively. The grey circles show sites with no statistically significant trend at 0.05 level.

To get a more detailed picture on how the tails of discharge distribution are changing, we investigate percent changes in the projected mean of 7-day low flows (Figures 2A and 2C) and 7-day high flows (Figures 2B and 2D) relative to the historical period. Figure 2 depicts that the magnitudes of 7-day low flows are projected to slightly decrease for both concentration paths relative to the baseline, and changes are marginally higher under the RCP 8.5 (Figure 2C). Considering the magnetite of 7-day high flows (Figures 2B and 2D), most locations exhibit pronounced increasing patterns. It is worth mentioning that the magnitude of change is higher under RCP 8.5 relative to RCP 4.5. Most of the stations that show slightly decreasing trends in the magnitude of 7-day high flows are located in the southern part of the study region.

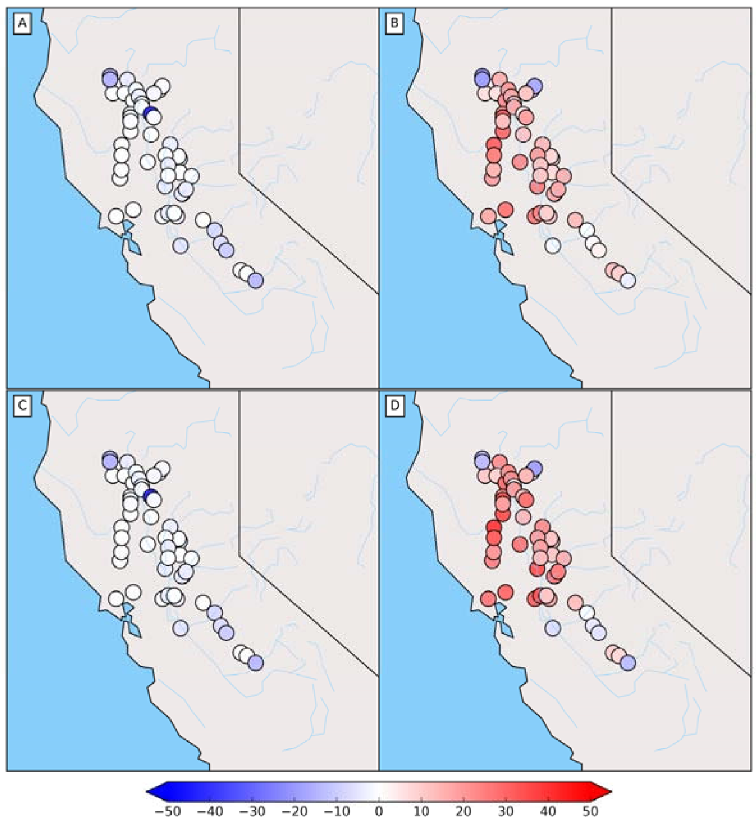

Figure 2: Percent change [%] in the magnitude of 7-day low flows (left panels) and 7-day high flows (right panels) relative to the historical period for the RCP 4.5 (top panels) and RCP 8.5 (bottom panels).

To this end, our analysis points to a decreasing trend in the magnitude of low flows and increasing trend in the magnitude of high flows. To further explore this issue, we investigate how the distribution of river discharge is expected to change under global warming. We extend our analysis to examine the presence of monotonic trends over different discharge quantiles (i.e., Q0.05, Q0.25, Q0.5, Q0.75, Q0.95) using the Mann-Kendall test. Here, we only show the results for RCP 8.5 for brevity, and similar results for RCP 4.5 can be found in Figure S3. Figure 3 shows that the future projections point to statistically significant decreasing trends in the streamflow relative to the baseline period for the 5th, 25th, 50th and 75th percentiles. While in the baseline period we do not observe a statistically significant change for the 95th percentiles of discharge, a significant increasing trend for the 95th percentile of projections is observed consistent with the previous figures. These trends are most prevalent over the northern part of the study area. Figure 3 confirms that current climate model simulations indicate an asymmetrical change in the tails of the streamflow distribution; i.e. low flows decrease and high flows increase.

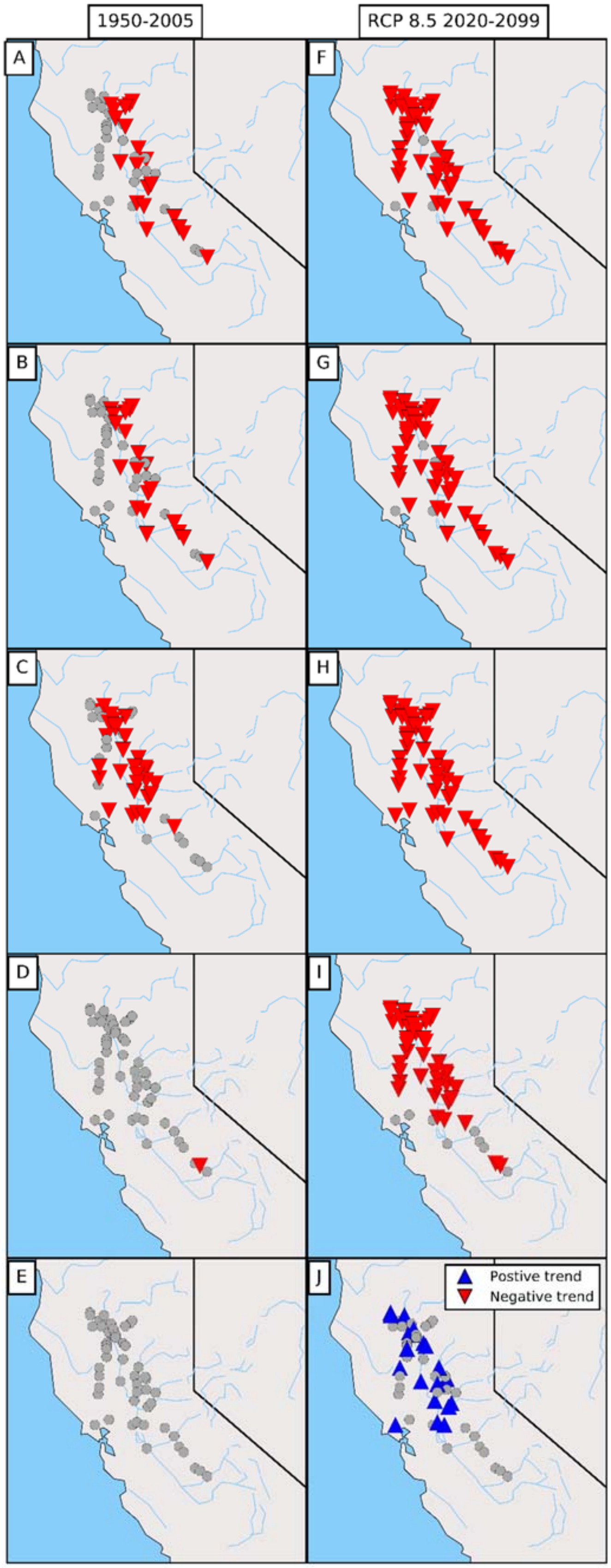
1950-2005
RCP 8.5 2020-2099
A
B
C
D
E
F
G
H
I
J
Postive trend
Negative trend

Figure 3: Trends in the magnitude of different discharge quantiles: Q0.05 (panels A and F), Q0.25 (panels B and G), Q0.50 (panels C and H), Q0.75 (panels D and I), and Q0.95 (panels E and J). Left panels depict the baseline period whereas the right panels represent future projections (RCP 8.5). Positive and negative trends are presented with upward blue, and downward red triangles, respectively. Grey circles show the sites with no statistically significant trends at 0.05 level.

The change in the distribution of streamflow is more evident by looking at Figure 4 which presents the Empirical Cumulative Distribution Functions (ECDFs) of the ensemble median of daily streamflow in the baseline and projection periods for two locations: Orville Lake (Figure 4A) and Shasta Lake (Figure 4B). The projected streamflow ECDFs confirm the results from Figure 3 and show the potential changes in different parts of the discharge distribution. The discharge below the 80th percentiles exhibits a lower low flow, while it indicates higher high flows above the 80th percentiles.

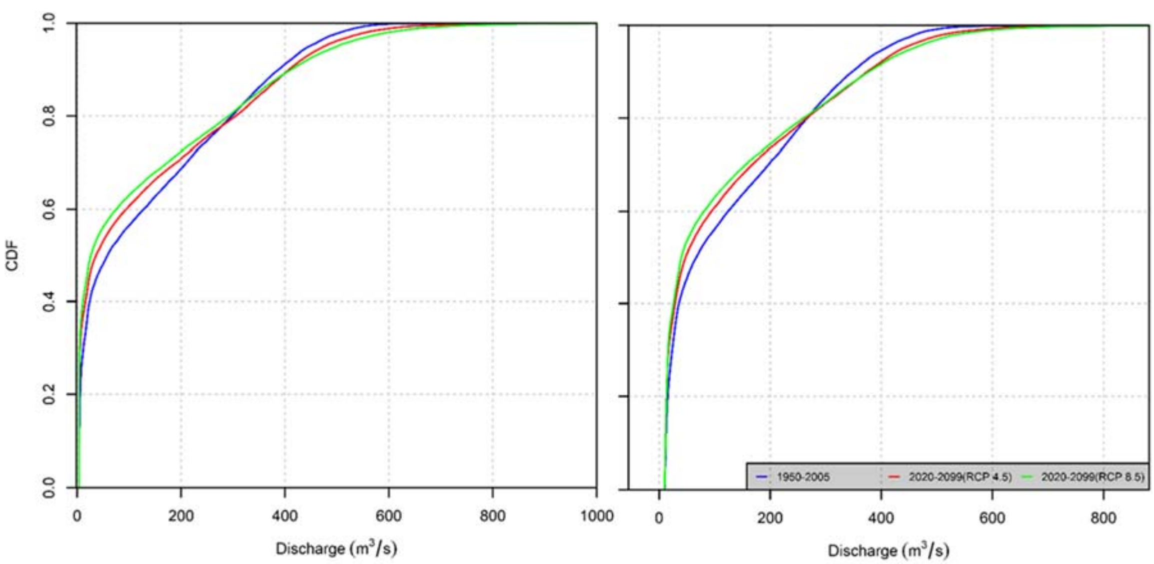

Figure 4: Empirical Cumulative Distribution Functions (ECDFs) of streamflow in the baseline (blue line) and projection periods (red line RCP 4.5 and green line RCP 8.5) in the Oroville Lake (left panel) and Shasta Lake (right panel).

To understand the seasonal changes, we have also investigated percent changes in the projected mean of streamflows relative to the baseline period at the monthly scale (Figures 5 and S4). During the winter months (December, January, and February) and March (when most of the annual precipitation is delivered), majority of the sites depict an increase in the monthly mean of projected streamflow. This increasing pattern is more prevalent for the sites that are located in the north part of the study region over the Sacramento River Basin. In the rest of the year (April to November), the results point to a marked decrease in the mean of streamflow relative to the baseline period, with deviation from the mean being more pronounced in April to July. Overall, these results show that mean monthly streamflows over the rainy season are projected to increase by the end of the century under RCP 8.5 (similar results for RCP 4.5 shown in Figure S4), while for the rest of the year a decreasing trend is expected. This indicates California can possibly face wetter wet seasons and drier dry seasons by the end of this century. This finding is in line with *Pierce et al. (2013)* that projected an increase in winter average precipitation in California. Note that these changes in the mean monthly streamflows are more noticeable for the higher emissions scenario (RCP 8.5; Figure S5).

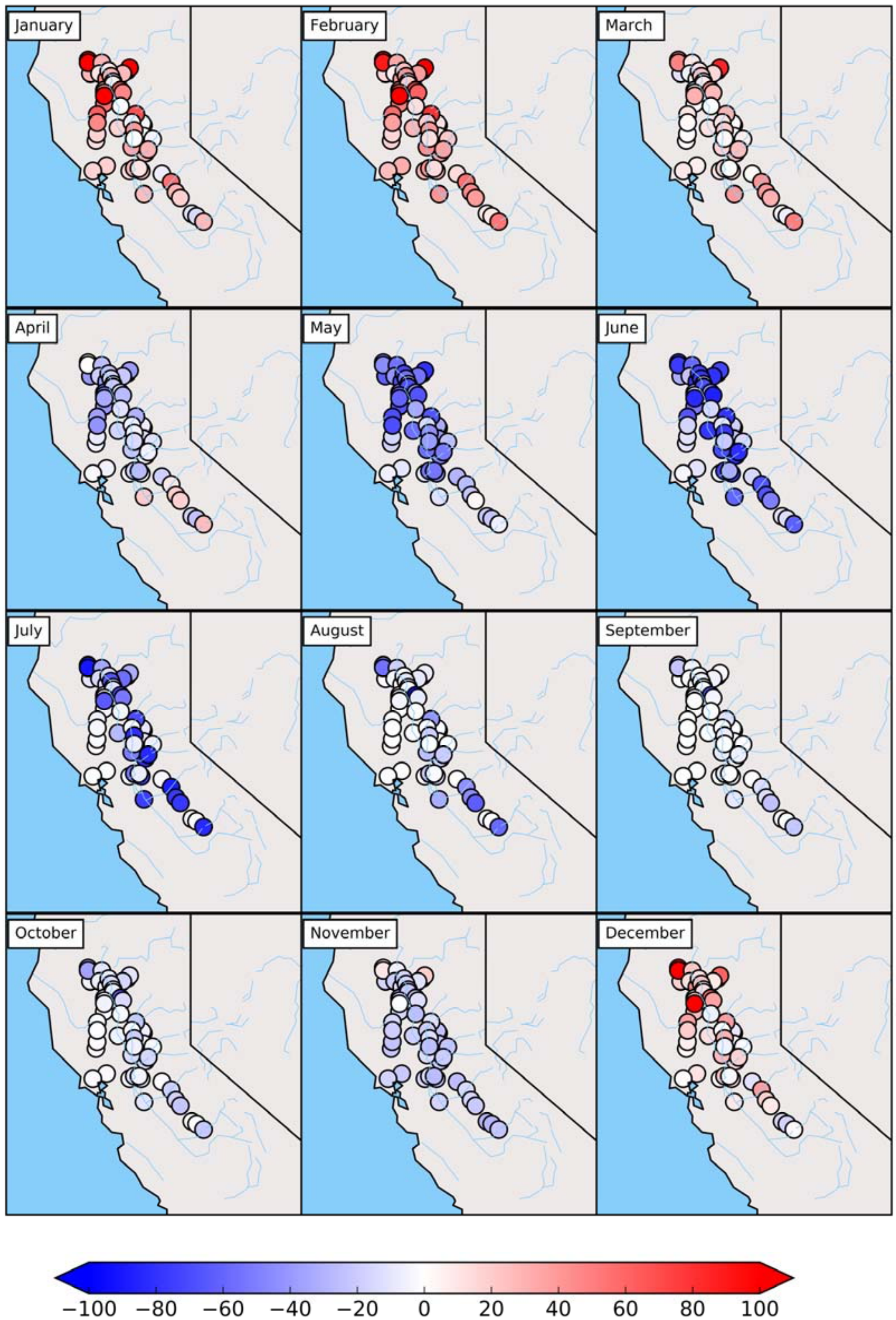

Figure 5: Percent change [%] in the mean of the monthly river discharge under RCP 8.5 relative to the baseline period.

4. Discussion and Conclusion

In this study, we explore potential changes in future river flows in California using bias-corrected and routed simulated streamflows from multi-model climate simulations. Our results indicate that the annual mean of daily streamflow is not expected to change significantly by the end of this century. However, we observe opposing trends and sign of change when examining changes in the upper and lower tails of streamflow distribution. Results point to a widespread statistically significant increase in the magnitude of the annual streamflow maxima and a prevalent decreasing trend in the annual streamflow minima under both RCP 4.5 and RCP 8.5 scenarios. Investigating 7-day low and high flows and different quantiles of streamflow distribution also confirm this finding, indicating that extreme high and low flows are expected to intensify while the mean flows are not expected to change significantly. Overall, the decreasing (increasing) trends in the magnitude of 7-day high flows are vivid in the southern (northern) part of the study domain. Our results are in agreement with *Yoon et al. (2015)* who postulated future changes in large scale circulation patterns might intensify future floods and droughts. Our findings are also consistent with *Li et al. (2017)* who pointed to declines in low to moderated discharge in the future. However, in contrast to *Li et al. (2017)*, our analysis does not identify a statistically significant change in the annual mean streamflow. Instead, we only find an increasing pattern in the magnitude of high flows.

We also examine projected changes in the mean of monthly streamflow relative to the baseline period. Model simulations show that while annual mean of daily streamflow is not projected to significantly change, mean of monthly streamflow is projected to increase during most of the rainy season (December to March) and to decrease in the dry season. This increasing signal is more pronounced for the sites that are located in the Sacramento River Basin. In other words, not only the distribution of streamflow, but also the seasonality of river discharge is projected to change by the end of this century. Note that, as *Wasko & Sharma (2017)* indicated, the response of streamflow to an extreme precipitation event depends on the catchment size, and extreme precipitation events at a higher temperature level may not necessarily result in higher streamflow. Our results here indicate that in the future, California can face wetter rainy seasons, and drier dry seasons as indicated. Moreover, *Das et al. (2011b)* have shown the important role of warm season warming versus cool season warming on the streamflow level in the western United States. They projected a higher reduction in streamflow under warmer warm season and an increase in the streamflow under warmer cool season. Therefore, projected changes in the mean of monthly streamflow will be of key importance for improving our strategies to manage water resources in California.

While attribution of the projected changes in discharge is not the main focus of this study, a possible explanation for the observed changes in river discharge is that low to moderate flow in rivers is sustained primarily by snow, with snowpack decreasing in the western United States and snowmelt happening earlier in spring (Huning & Margulis, 2017; Maurer et al., 2007; Mote et al., 2005; Stewart et al., 2005). *Stewart et al. (2005)* examined the seasonality of streamflow in snowmelt-dominated regions of western North America from 1948 to 2002 where they pointed to a reduction of spring and summer streamflow due to earlier snowmelt. For the northern part of California, Pierce et al. (2013) projected an increase in daily precipitation intensity in the winter season while spring precipitation is projected to decrease that can worsen the impact of earlier snowpack melting on the water resources. A smaller contribution of snowmelt to streamflow and also reduction in the ratio of snow over rain can lead to lower low to moderate discharge during seasons with lower precipitation (Li et al., 2017; Mote et al., 2005). Moreover, *Diffenbaugh et al. (2015)* indicated that snowpack in the montane regions of California has an important role in sustaining river discharge during the dry season. However, the projected increase in temperatures, and consequently earlier snowmelt can result in elongated dry and low flow periods (Ashfaq et al., 2013; Diffenbaugh et al., 2015; Li et al., 2017; Stewart et al., 2005). *Li et al. (2017)* showed that historically one-third of precipitation over the entire western United States falls as snow, which accounts for more than half of the total annual streamflow. They projected that smaller fraction (~%40 to %30) of snowmelt will contribute to annual discharge in the future. Furthermore, they argued that runoff will be more rainfall driven in the future over California. On the other hand, high flow events might be mainly controlled by moist and warm extreme AR events (M. Dettinger, 2011; Jeon et al., 2015). An extensive discussion on the impacts of warming climate on ARs can be found in *Espinoza et al. (2018)* where they indicated that all the studies conducted over western United States point to an increase in the frequency of AR events in a changing climate. Moreover, in a recent study, *Ragno et al., (2018)* showed that future extreme precipitation events are expected to intensify in California, despite relatively unchanged precipitation mean. Their findings are consistent with our results on future changes to the high flows.

Projected changes in California’s streamflows can have profound implications for water resource management and infrastructure design and risk assessment. This issue becomes even more important considering the already aging infrastructures (e.g., dams, levees, and bridges) designed based on historical extremes and the assumption of stationarity. Any shift in high flows in the future would increase the risk of infrastructure failure or damages to critical structures such as the 2017 failure of the Orville Dam spillway. Therefore, new methodological frameworks are needed to incorporate potential projected changes in the current infrastructure design and risk assessment procedures to lower the risk of infrastructure failures in the future.

Acknowledgments

This study was partially supported by the California Energy Commission grant (500-15-005) and the United States National Science Foundation award CMMI-1635797. We acknowledge the World Climate Research Programmes Working Group on Coupled Modeling, which is responsible for CMIP, and we thank the climate-modeling groups for producing and making available their model output. For CMIP, the U.S. Department of Energy's Program for Climate Model Diagnosis and Intercomparison (PCMDI) provides coordinating support and leads the development of software infrastructure in partnership with the Global Organization for Earth System Science Portals. We also thank Daniel Cayan, David Pierce, and Julie Kalansky from Scripps Institution of Oceanography, University of California, San Diego, for providing downscaled and routed runoff projections over California (http://loca.ucsd.edu/).

References

AghaKouchak, A., Cheng, L., Mazdiyasni, O., & Farahmand, A. (2014). Global warming and changes in risk of concurrent climate extremes: Insights from the 2014 California drought. *Geophysical Research Letters*, *41*(24), 2014GL062308. https://doi.org/10.1002/2014GL062308

Alfieri, L., Burek, P., Feyen, L., & Forzieri, G. (2015). Global warming increases the frequency of river floods in Europe. *Hydrol. Earth Syst. Sci.*, *19*(5), 2247–2260. https://doi.org/10.5194/hess-19-2247-2015

Ashfaq, M., Ghosh, S., Kao, S.-C., Bowling, L. C., Mote, P., Touma, D., et al. (2013). Near-term acceleration of hydroclimatic change in the western U.S. *Journal of Geophysical Research: Atmospheres*, *118*(19), 10,676-10,693. https://doi.org/10.1002/jgrd.50816

Barth, N. A., Villarini, G., NAyak, M., & White, K. (2016). Mixed populations and annual flood frequency estimates in the western United States: The role of atmospheric rivers. *Water Resources Research*, n/a-n/a. https://doi.org/10.1002/2016WR019064

Beighley, R. E., Melack, J. M., & Dunne, T. (2003). Impacts of California's Climatic Regimes and Coastal Land Use Change on Streamflow Characteristics1. *JAWRA Journal of the American Water Resources Association*, *39*(6), 1419–1433. https://doi.org/10.1111/j.1752-1688.2003.tb04428.x

Berghuijs, W. R., Woods, R. A., & Hrachowitz, M. (2014). A precipitation shift from snow towards rain leads to a decrease in streamflow. *Nature Climate Change*, *4*(7), 583–586. https://doi.org/10.1038/nclimate2246

Burke, W. D., & Ficklin, D. L. (2017). Future projections of streamflow magnitude and timing differ across coastal watersheds of the western United States: PROJECTED STREAMFLOW MAGNITUDE AND TIMING IN THE COASTAL WESTERN US. *International Journal of Climatology*. https://doi.org/10.1002/joc.5099

Cayan, D. R., Dettinger, M. D., Kammerdiener, S. A., Caprio, J. M., & Peterson, D. H. (2001). Changes in the Onset of Spring in the Western United States. *Bulletin of the American Meteorological Society*, *82*(3), 399–415. https://doi.org/10.1175/1520-0477(2001)082<0399:CITOOS>2.3.CO;2

CDWR. (2015). Perspectives and Guidance for Climate Change Analysis. California Department of Water Resources and Climate Change Technical Advisory Group. Retrieved from http://www.water.ca.gov/climatechange/docs/2015/Perspectives_Guidance_Climate_Change_Analysis.pdf

Cheng, L., AghaKouchak, A., Gilleland, E., & Katz, R. W. (2014). Non-stationary extreme value analysis in a changing climate. *Climatic Change*, *127*(2), 353–369. https://doi.org/10.1007/s10584-014-1254-5

Das, T., Dettinger, M. D., Cayan, D. R., & Hidalgo, H. G. (2011a). Potential increase in floods in California's Sierra Nevada under future climate projections. *Climatic Change*, *109*(1), 71–94. https://doi.org/10.1007/s10584-011-0298-z

Das, T., Pierce, D. W., Cayan, D. R., Vano, J. A., & Lettenmaier, D. P. (2011b). The importance of warm season warming to western U.S. streamflow changes: WARM SEASON WARMING STREAMFLOW CHANGES. *Geophysical Research Letters*, *38*(23), n/a-n/a. https://doi.org/10.1029/2011GL049660

Das, T., Maurer, E. P., Pierce, D. W., Dettinger, M. D., & Cayan, D. R. (2013). Increases in flood magnitudes in California under warming climates. *Journal of Hydrology*, *501*, 101–110. https://doi.org/10.1016/j.jhydrol.2013.07.042

Demaria, E. M. C., Palmer, R. N., & Roundy, J. K. (2016). Regional climate change projections of streamflow characteristics in the Northeast and Midwest U.S. *Journal of Hydrology: Regional Studies*, *5*, 309–323. https://doi.org/10.1016/j.ejrh.2015.11.007

Dettinger, M. (2011). Climate Change, Atmospheric Rivers, and Floods in California - A Multimodel Analysis of Storm Frequency and Magnitude Changes1: Climate Change, Atmospheric Rivers, and Floods in California - A Multimodel Analysis of Storm Frequency and Magnitude Changes. *JAWRA Journal of the American Water Resources Association*, *47*(3), 514–523. https://doi.org/10.1111/j.1752-1688.2011.00546.x

Dettinger, M. D., & Ingram, B. L. (2012). The Coming Megafloods. *Scientific American*, *308*(1), 64–71. https://doi.org/10.1038/scientificamerican0113-64

Diffenbaugh, N. S., Swain, D. L., & Touma, D. (2015). Anthropogenic warming has increased drought risk in California. *Proceedings of the National Academy of Sciences*, *112*(13), 3931–3936. https://doi.org/10.1073/pnas.1422385112

Espinoza, V., Waliser, D. E., Guan, B., Lavers, D. A., & Ralph, F. M. (2018). Global Analysis of Climate Change Projection Effects on Atmospheric Rivers. *Geophysical Research Letters*, *45*(9), 4299–4308. https://doi.org/10.1029/2017GL076968

Hailegeorgis, T. T., & Alfredsen, K. (2017). Regional flood frequency analysis and prediction in ungauged basins including estimation of major uncertainties for mid-Norway. *Journal of Hydrology: Regional Studies*, *9*, 104–126. https://doi.org/10.1016/j.ejrh.2016.11.004

Hardin, E., AghaKouchak, A., Qomi, M. J. A., Madani, K., Tarroja, B., Zhou, Y., et al. (2017). California drought increases CO2 footprint of energy. *Sustainable Cities and Society*, *28*, 450–452. https://doi.org/10.1016/j.scs.2016.09.004

Harpold, A. A., Rajagopal S., Crews J. B., Winchell T., & Schumer R. (2017). Relative Humidity Has Uneven Effects on Shifts From Snow to Rain Over the Western U.S. *Geophysical Research Letters*, *44*(19), 9742–9750. https://doi.org/10.1002/2017GL075046

Helsel, D. R., & Hirsch, R. M. (1992). *Statistical methods in water resources*. Amsterdam: Elsevier.

Huning, L. S., & Margulis, S. A. (2017). Climatology of seasonal snowfall accumulation across the Sierra Nevada (USA): Accumulation rates, distributions, and variability. *Water Resources Research*, *53*(7), 6033–6049. https://doi.org/10.1002/2017WR020915

Jeon, S., Prabhat, Byna, S., Gu, J., Collins, W. D., & Wehner, M. F. (2015). Characterization of extreme precipitation within atmospheric river events over California. *Advances in Statistical Climatology, Meteorology and Oceanography*, *1*(1), 45–57. https://doi.org/10.5194/ascmo-1-45-2015

Kendall, M. G., & Gibbons, J. D. (1990). *Rank correlation methods* (5th ed). London : New York, NY: E. Arnold ; Oxford University Press.

Knowles, N., Dettinger, M. D., & Cayan, D. R. (2006). Trends in Snowfall versus Rainfall in the Western United States. *Journal of Climate*, *19*(18), 4545–4559. https://doi.org/10.1175/JCLI3850.1

Koutsoyiannis, D. (2006). Nonstationarity versus scaling in hydrology. *Journal of Hydrology*, *324*(1–4), 239–254. https://doi.org/10.1016/j.jhydrol.2005.09.022

Krakauer, N. Y., & Fung, I. (2008). Mapping and attribution of change in streamflow in the coterminous United States. *Hydrol. Earth Syst. Sci.*, *12*(4), 1111–1120. https://doi.org/10.5194/hess-12-1111-2008

Leung, L. R., & Qian, Y. (2009). Atmospheric rivers induced heavy precipitation and flooding in the western U.S. simulated by the WRF regional climate model: ATMOSPHERIC RIVER, PRECIPITATION, FLOOD. *Geophysical Research Letters*, *36*(3), n/a-n/a. https://doi.org/10.1029/2008GL036445

Li, D., Wrzesien, M. L., Durand, M., Adam, J., & Lettenmaier, D. P. (2017). How much runoff originates as snow in the western United States, and how will that change in the future? *Geophysical Research Letters*, *44*(12), 2017GL073551. https://doi.org/10.1002/2017GL073551

Lins, H. F., & Slack, J. R. (1999). Streamflow trends in the United States. *Geophysical Research Letters*, *26*(2), 227–230. https://doi.org/10.1029/1998GL900291

Livneh, B., Rosenberg, E. A., Lin, C., Nijssen, B., Mishra, V., Andreadis, K. M., et al. (2013). A Long-Term Hydrologically Based Dataset of Land Surface Fluxes and States for the Conterminous United States: Update and Extensions. *Journal of Climate*, *26*(23), 9384–9392. https://doi.org/10.1175/JCLI-D-12-00508.1

Luke, A., Vrugt, J. A., AghaKouchak, A., Matthew, R., & Sanders, B. F. (2017). Predicting nonstationary flood frequencies: Evidence supports an updated stationarity thesis in the United States. *Water Resources Research*, *53*(7), 5469–5494. https://doi.org/10.1002/2016WR019676

Mallakpour, I., & Villarini, G. (2015). The changing nature of flooding across the central United States. *Nature Climate Change*, *5*(3), 250–254. https://doi.org/10.1038/nclimate2516

Mallakpour, I., Villarini, G., Jones, M. P., & Smith, J. A. (2017). On the use of Cox regression to examine the temporal clustering of flooding and heavy precipitation across the central United States. *Global and Planetary Change*, *155*, 98–108. https://doi.org/10.1016/j.gloplacha.2017.07.001

Mann, H. B. (1945). Nonparametric Tests Against Trend. *Econometrica*, *13*(3), 245. https://doi.org/10.2307/1907187

Mao, Y., Nijssen, B., & Lettenmaier, D. P. (2015). Is climate change implicated in the 2013–2014 California drought? A hydrologic perspective. *Geophysical Research Letters*, *42*(8), 2015GL063456. https://doi.org/10.1002/2015GL063456

Maurer, E. P., Wood, A. W., Adam, J. C., Lettenmaier, D. P., & Nijssen, B. (2002). A Long-Term Hydrologically Based Dataset of Land Surface Fluxes and States for the Conterminous United States*. *Journal of Climate*, *15*(22), 3237–3251. https://doi.org/10.1175/1520-0442(2002)015<3237:ALTHBD>2.0.CO;2

Maurer, E. P., Stewart, I. T., Bonfils, C., Duffy, P. B., & Cayan, D. (2007). Detection, attribution, and sensitivity of trends toward earlier streamflow in the Sierra Nevada. *Journal of Geophysical Research*, *112*(D11). https://doi.org/10.1029/2006JD008088

McCabe, G. J., & Wolock, D. M. (2014). Spatial and temporal patterns in conterminous United States streamflow characteristics. *Geophysical Research Letters*, *41*(19), 2014GL061980. https://doi.org/10.1002/2014GL061980

Mehrotra, R., & Sharma, A. (2012). An improved standardization procedure to remove systematic low frequency variability biases in GCM simulations: TECHNICAL NOTE. *Water Resources Research*, *48*(12). https://doi.org/10.1029/2012WR012446

Mehrotra, R., & Sharma, A. (2015). Correcting for systematic biases in multiple raw GCM variables across a range of timescales. *Journal of Hydrology*, *520*, 214–223. https://doi.org/10.1016/j.jhydrol.2014.11.037

Mehrotra, R., & Sharma, A. (2016). A Multivariate Quantile-Matching Bias Correction Approach with Auto- and Cross-Dependence across Multiple Time Scales: Implications for Downscaling. *Journal of Climate*, *29*(10), 3519–3539. https://doi.org/10.1175/JCLI-D-15-0356.1

Milly, P. C. D., Dunne, K. A., & Vecchia, A. V. (2005). Global pattern of trends in streamflow and water availability in a changing climate. *Nature*, *438*(7066), 347–350. https://doi.org/10.1038/nature04312

Monk, W. A., Wood, P. J., Hannah, D. M., & Wilson, D. A. (2007). Selection of river flow indices for the assessment of hydroecological change. *River Research and Applications*, *23*(1), 113–122. https://doi.org/10.1002/rra.964

Mote, P. W., Hamlet, A. F., Clark, M. P., & Lettenmaier, D. P. (2005). Declining mountain snowpack in western north America. *Bulletin of the American Meteorological Society*, *86*(1), 39–50. https://doi.org/10.1175/BAMS-86-1-39

Nazemi, A. & Wheater, H. S. (2014). Assessing the Vulnerability of Water Supply to Changing Streamflow Conditions. *Eos, Transactions American Geophysical Union*, *95*(32), 288–288. https://doi.org/10.1002/2014EO320007

Neelin, J. D., Langenbrunner, B., Meyerson, J. E., Hall, A., & Berg, N. (2013). California Winter Precipitation Change under Global Warming in the Coupled Model Intercomparison Project Phase 5 Ensemble. *Journal of Climate*, *26*(17), 6238–6256. https://doi.org/10.1175/JCLI-D-12-00514.1

O'Gorman, P. A., & Muller, C. J. (2010). How closely do changes in surface and column water vapor follow Clausius–Clapeyron scaling in climate change simulations? *Environmental Research Letters*, *5*(2), 025207. https://doi.org/10.1088/1748-9326/5/2/025207

Olden, J. D., & Poff, N. L. (2003). Redundancy and the choice of hydrologic indices for characterizing streamflow regimes. *River Research and Applications*, *19*(2), 101–121. https://doi.org/10.1002/rra.700

Pachauri, R. K., Mayer, L., & Intergovernmental Panel on Climate Change (Eds.). (2015). *Climate change 2014: synthesis report*. Geneva, Switzerland: Intergovernmental Panel on Climate Change.

Payne, A. E., & Magnusdottir, G. (2015). An evaluation of atmospheric rivers over the North Pacific in CMIP5 and their response to warming under RCP 8.5: NORTH PACIFIC ATMOSPHERIC RIVERS IN CMIP5. *Journal of Geophysical Research: Atmospheres*, *120*(21), 11,173-11,190. https://doi.org/10.1002/2015JD023586

Pierce, D., Cayan, D., & Dehann, L. (2016). Creating Climate projections to support the 4th California Climate Assessment. Division of Climate, Atmospheric Sciences, and Physical Oceanography Scripps Institution of Oceanography, La Jolla, CA. Retrieved from http://docketpublic.energy.ca.gov/PublicDocuments/16-IEPR-

04/TN211805_20160614T101821_Creating_Climate_projections_to_support_the_4th_California_Clim.pdf

Pierce, D. W., Cayan, D. R., Das, T., Maurer, E. P., Miller, N. L., Bao, Y., et al. (2013). The Key Role of Heavy Precipitation Events in Climate Model Disagreements of Future Annual Precipitation Changes in California. *Journal of Climate*, *26*(16), 5879–5896. https://doi.org/10.1175/JCLI-D-12-00766.1

Pierce, D. W., Cayan, D. R., & Thrasher, B. L. (2014). Statistical Downscaling Using Localized Constructed Analogs (LOCA). *Journal of Hydrometeorology*, *15*(6), 2558–2585. https://doi.org/10.1175/JHM-D-14-0082.1

Pierce, D. W., Cayan, D. R., Maurer, E. P., Abatzoglou, J. T., & Hegewisch, K. C. (2015). Improved Bias Correction Techniques for Hydrological Simulations of Climate Change*. *Journal of Hydrometeorology*, *16*(6), 2421–2442. https://doi.org/10.1175/JHM-D-14-0236.1

Ragno, E., AghaKouchak, A., Love, C. A., Cheng, L., Vahedifard, F., & Lima, C. H. R. (2018). Quantifying Changes in Future Intensity-Duration-Frequency Curves Using Multimodel Ensemble Simulations: EXTREMES IN WARMING CLIMATE. *Water Resources Research*, *54*(3), 1751–1764. https://doi.org/10.1002/2017WR021975

Ralph, F. M., Coleman, T., Neiman, P. J., Zamora, R. J., & Dettinger, M. D. (2013). Observed Impacts of Duration and Seasonality of Atmospheric-River Landfalls on Soil Moisture and Runoff in Coastal Northern California. *Journal of Hydrometeorology*, *14*(2), 443–459. https://doi.org/10.1175/JHM-D-12-076.1

Read, L. K., & Vogel, R. M. (2015). Reliability, return periods, and risk under nonstationarity. *Water Resources Research*, *51*(8), 6381–6398. https://doi.org/10.1002/2015WR017089

Regonda, S. K., Rajagopalan, B., Clark, M., & Pitlick, J. (2005). Seasonal Cycle Shifts in Hydroclimatology over the Western United States. *Journal of Climate*, *18*(2), 372–384. https://doi.org/10.1175/JCLI-3272.1

Richter, B. D., Baumgartner, J. V., Powell, J., & Braun, D. P. (1996). A Method for Assessing Hydrologic Alteration within Ecosystems. *Conservation Biology*, *10*(4), 1163–1174. https://doi.org/10.1046/j.1523-1739.1996.10041163.x

Richter, B. D., Baumgartner, J. V., Braun, D. P., & Powell, J. (1998). A spatial assessment of hydrologic alteration within a river network. *Regulated Rivers: Research & Management*, *14*(4), 329–340. https://doi.org/10.1002/(SICI)1099-1646(199807/08)14:4<329::AID-RRR505>3.0.CO;2-E

Sadegh, M., Vrugt, J. A., Xu, C., & Volpi, E. (2015). The stationarity paradigm revisited: Hypothesis testing using diagnostics, summary metrics, and DREAM $_{(ABC)}$: REVISITING SATIONARITY PARADIGM. *Water Resources Research*, *51*(11), 9207–9231. https://doi.org/10.1002/2014WR016805

Scheff, J., & Frierson, D. M. W. (2014). Scaling Potential Evapotranspiration with Greenhouse Warming. *Journal of Climate*, *27*(4), 1539–1558. https://doi.org/10.1175/JCLI-D-13-00233.1

Shukla, S., Safeeq, M., AghaKouchak, A., Guan, K., & Funk, C. (2015). Temperature impacts on the water year 2014 drought in California. *Geophysical Research Letters*, *42*(11), 2015GL063666. https://doi.org/10.1002/2015GL063666

Stewart, I. T., Cayan, D. R., & Dettinger, M. D. (2005). Changes toward Earlier Streamflow Timing across Western North America. *Journal of Climate*, *18*(8), 1136–1155. https://doi.org/10.1175/JCLI3321.1

Thorne, J. H., Boynton, R. M., Flint, L. E., & Flint, A. L. (2015). The magnitude and spatial patterns of historical and future hydrologic change in California's watersheds. *Ecosphere*, *6*(2), 1–30. https://doi.org/10.1890/ES14-00300.1

Vahedifard, F., AghaKouchak, A., Ragno, E., Shahrokhabadi, S., & Mallakpour, I. (2017). Lessons from the Oroville dam. *Science*, *355*(6330), 1139. https://doi.org/10.1126/science.aan0171

Villarini, G., & Strong, A. (2014). Roles of climate and agricultural practices in discharge changes in an agricultural watershed in Iowa. *Agriculture, Ecosystems & Environment*, *188*, 204–211. https://doi.org/10.1016/j.agee.2014.02.036

Villarini, G., Serinaldi, F., Smith, J. A., & Krajewski, W. F. (2009). On the stationarity of annual flood peaks in the continental United States during the 20th century. *Water Resources Research*, *45*(8), W08417. https://doi.org/10.1029/2008WR007645

Villarini, G., Scoccimarro, E., White, K. D., Arnold, J. R., Schilling, K. E., & Ghosh, J. (2015). Projected Changes in Discharge in an Agricultural Watershed in Iowa. *JAWRA Journal of the American Water Resources Association*, *51*(5), 1361–1371. https://doi.org/10.1111/1752-1688.12318

Voss, R., May, W., & Roeckner, E. (2002). Enhanced resolution modelling study on anthropogenic climate change: changes in extremes of the hydrological cycle. *International Journal of Climatology*, *22*(7), 755–777. https://doi.org/10.1002/joc.757

Wang, G., Wang, D., Trenberth, K. E., Erfanian, A., Yu, M., Bosilovich, M. G., & Parr, D. T. (2017). The peak structure and future changes of the relationships between extreme precipitation and temperature. *Nature Climate Change*, *advance online publication*. https://doi.org/10.1038/nclimate3239

Wasko, C., & Sharma, A. (2017). Global assessment of flood and storm extremes with increased temperatures. *Scientific Reports*, *7*(1). https://doi.org/10.1038/s41598-017-08481-1

Yoon, J.-H., Wang, S.-Y. S., Gillies, R. R., Kravitz, B., Hipps, L., & Rasch, P. J. (2015). Increasing water cycle extremes in California and in relation to ENSO cycle under global warming. *Nature Communications*, *6*, ncomms9657. https://doi.org/10.1038/ncomms9657

Zhu, T., Jenkins, M. W., & Lund, J. R. (2005). Estimated Impacts of Climate Warming on California Water Availability Under Twelve Future Climate Scenarios1. *JAWRA Journal of the American Water Resources Association*, *41*(5), 1027–1038. https://doi.org/10.1111/j.1752-1688.2005.tb03783.x

Supplementary Materials:

Table S1: List of the global climate models used in this study.

models	model name
m1	ACCESS1
m2	CanESM2
m3	CCSM4
m4	CESM1-BGC
m5	CMCC-CMS
m6	CNRM-CM5
m7	GFDL-CM3
m8	HadGEM2-CC
m9	HadGEM2-ES
m10	MIROC5

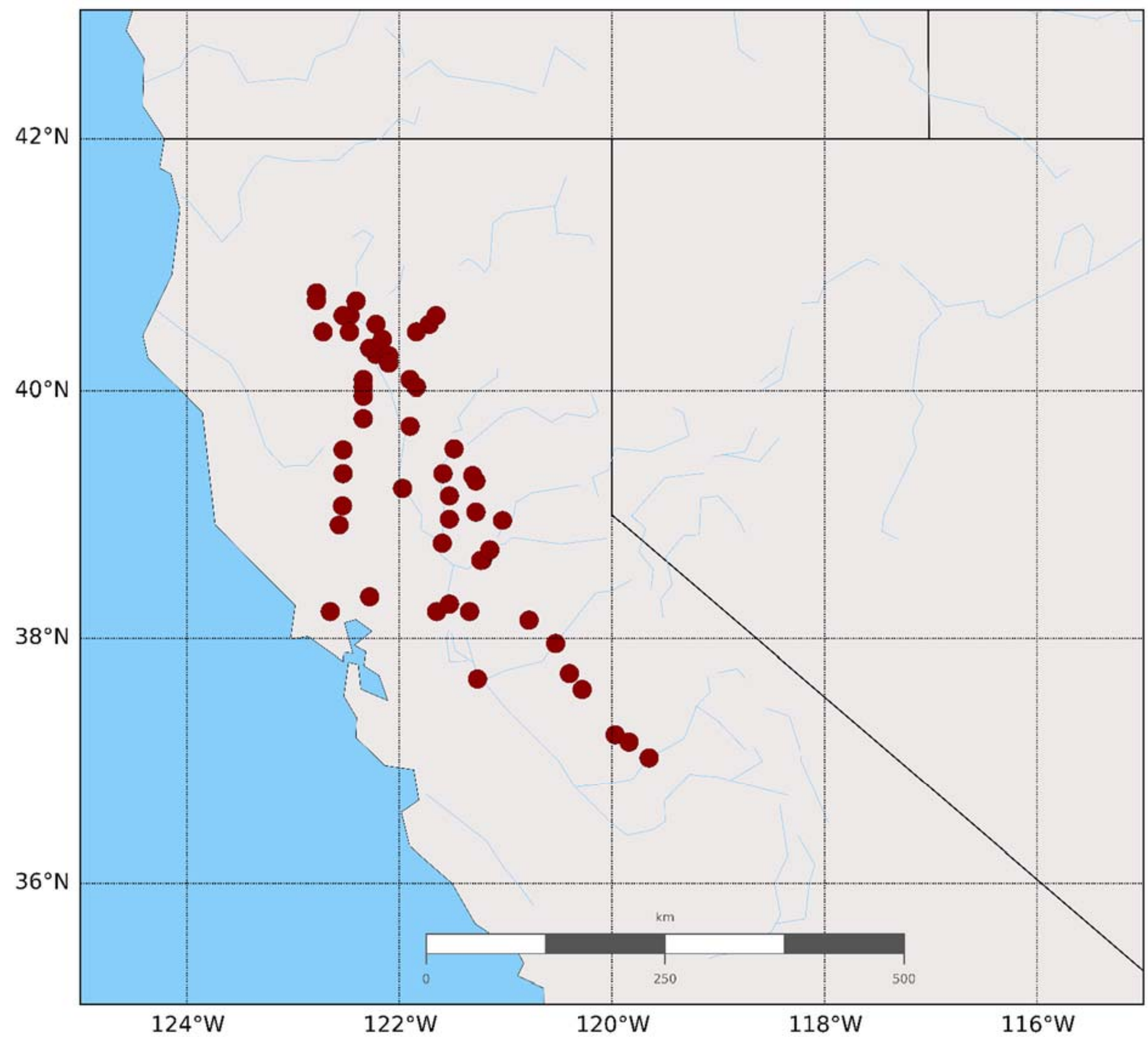

Figure S1: Map showing location of the study area. The dark red circles show the location of the 59 routed streamflow sites used in this study.

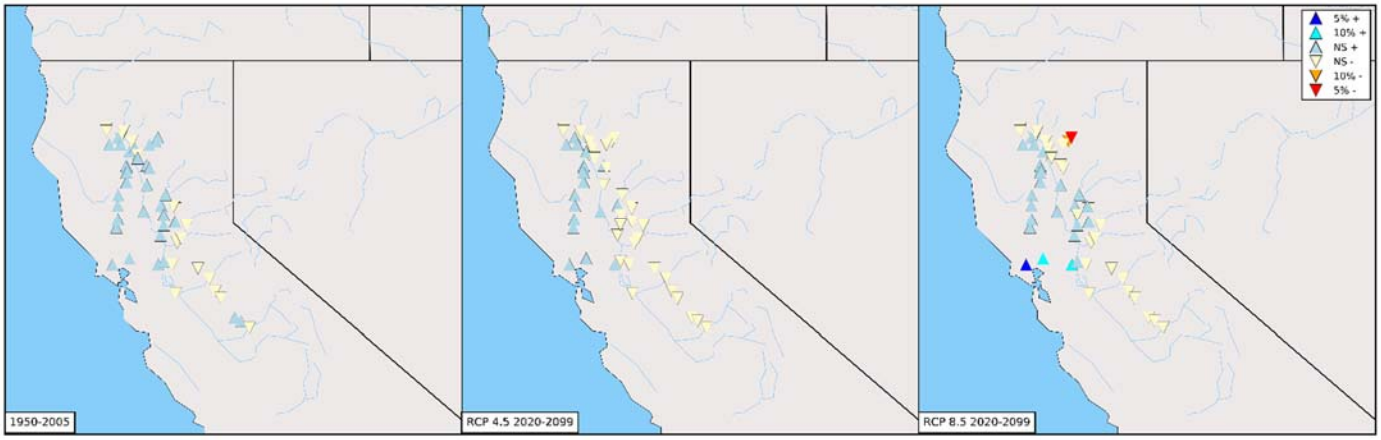

Figure S2: Same as Figure 1 in the main paper but for the annual volume of water $[\frac{m^3}{s}]$. In this figure, the dark blue (cyan) upward triangles show a statistically significant increasing trend at the 5% (10%) level and the red (orange) downward triangles show a statistically significant decreasing trend at the 5% (10%) level. The light blue (cream) triangles show the locations with increasing (decreasing) trends that are not statistically significant at 10% level.

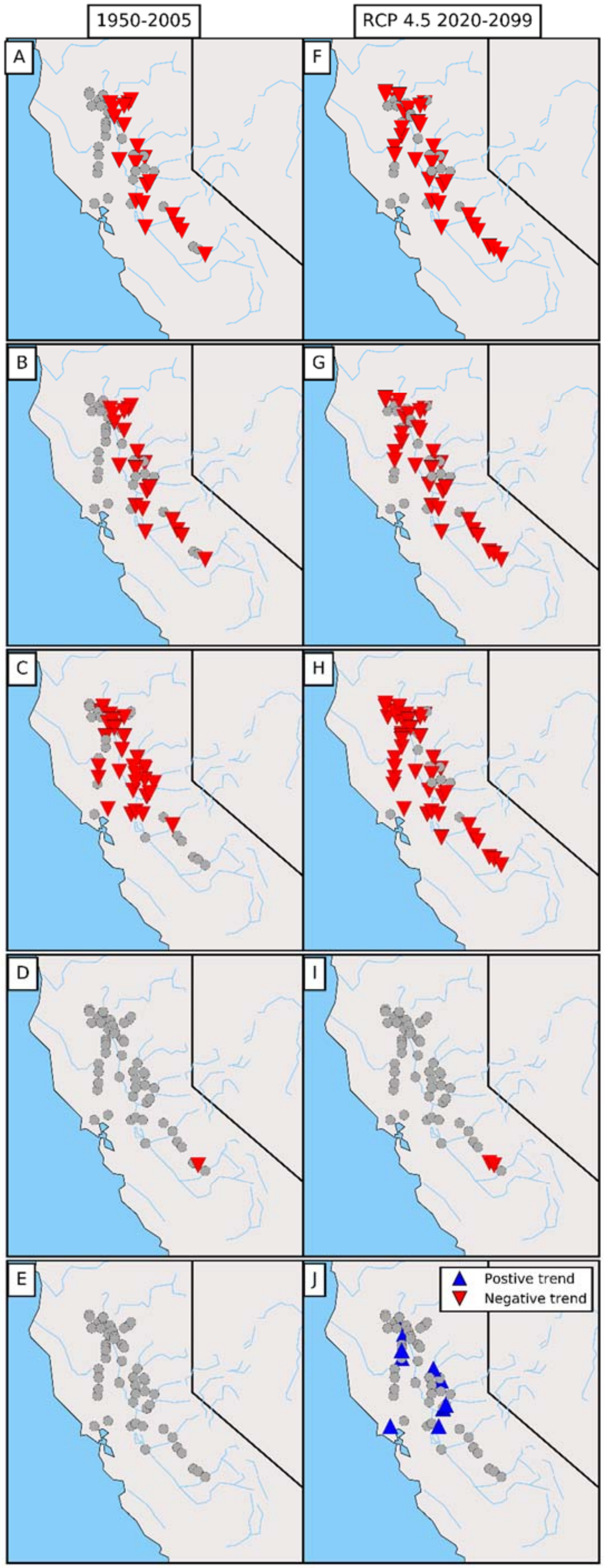
1950-2005
RCP 4.5 2020-2099
A
B
C
D
E
F
G
H
I
J
Postive trend
Negative trend

649

Figure S3: Same as Figure 3 in the main text but for the RCP 4.5 scenario.

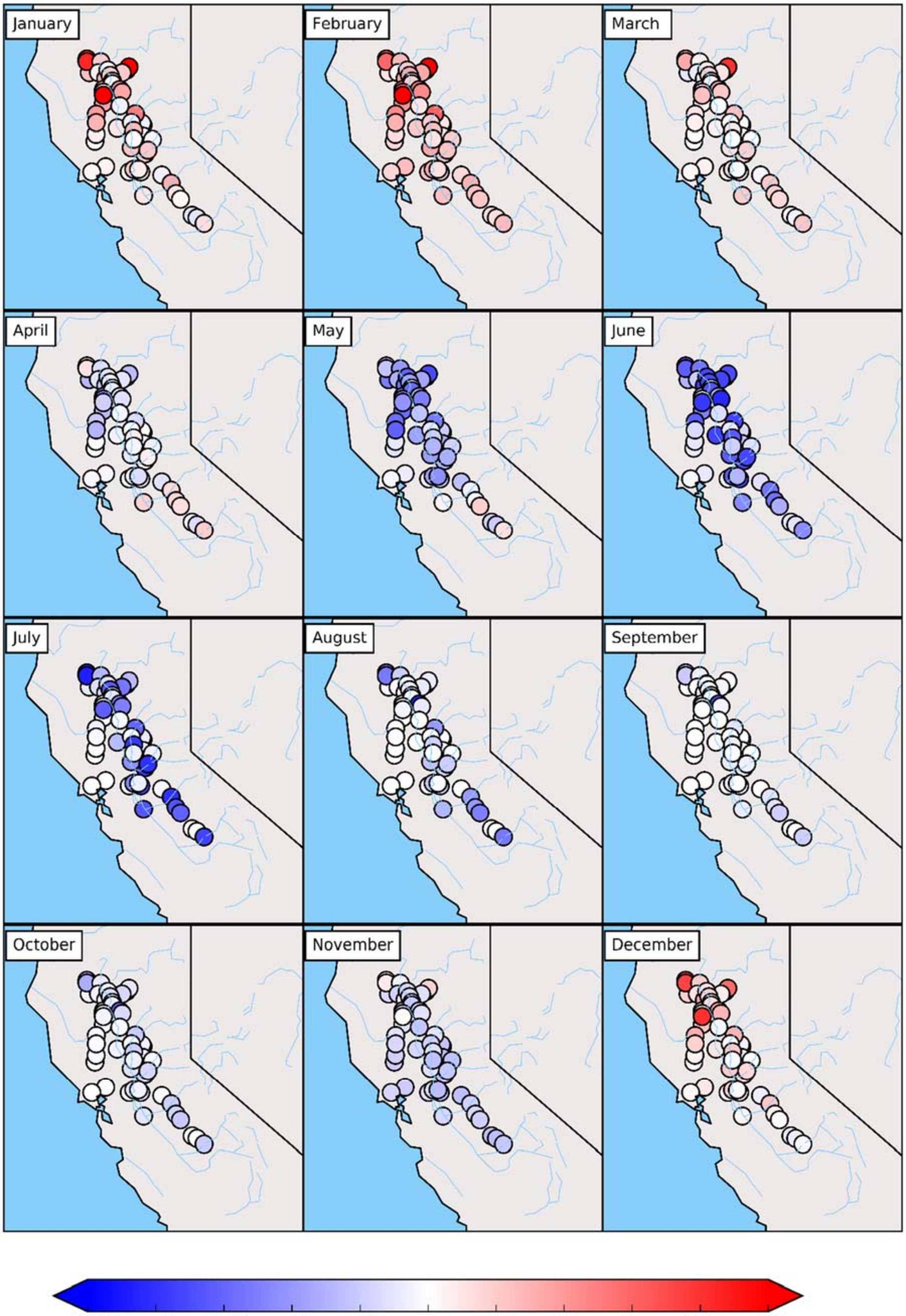
January
February
March
April
May
June
July
August
September
October
November
December
−100
−80
−60
−40
−20
0
20
40
60
80
100

652

Figure S4: Same as Figure 5 in the main paper but for the RCP 4.5 scenario.

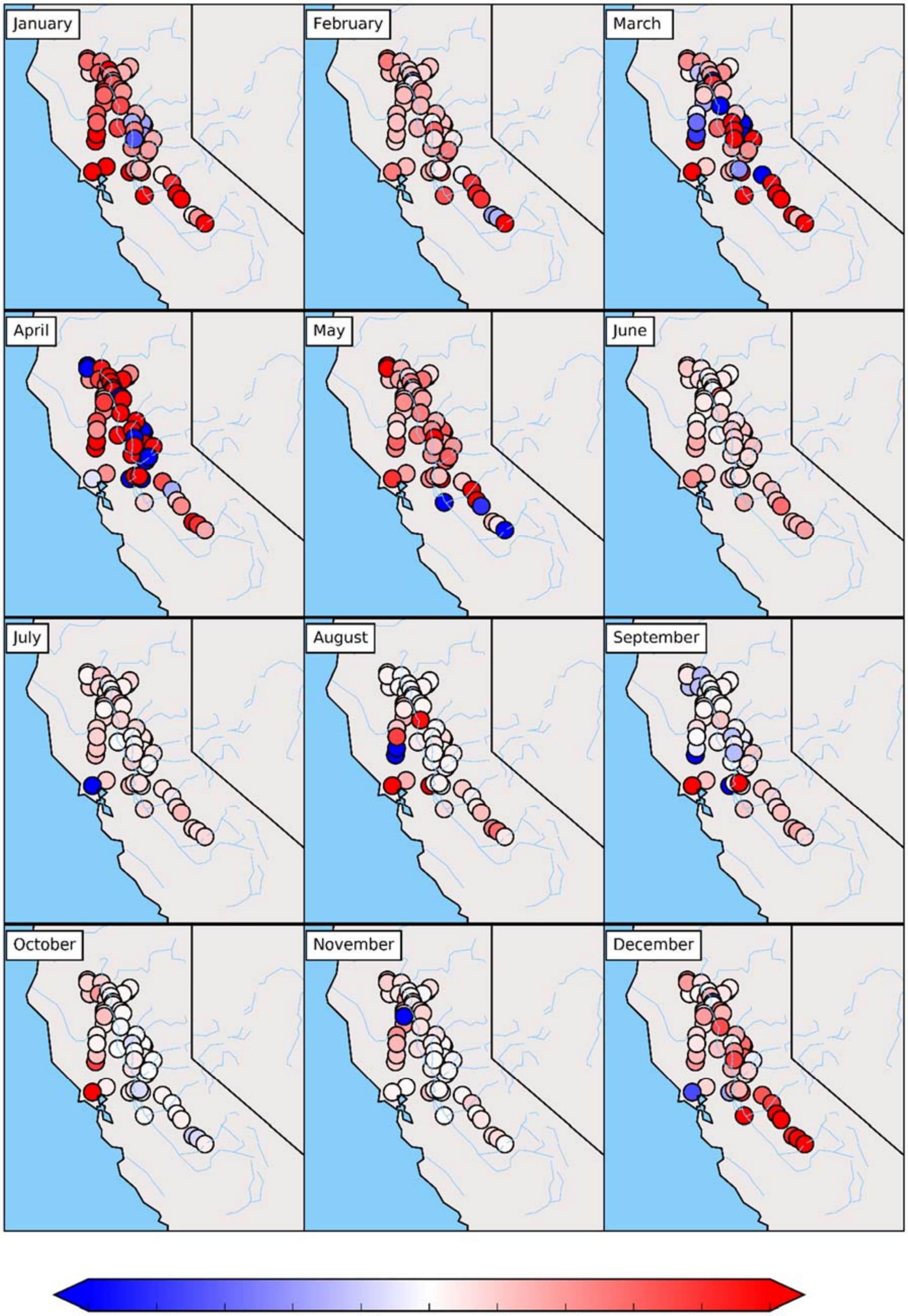
January
February
March
April
May
June
July
August
September
October
November
December
−100
−80
−60
−40
−20
0
20
40
60
80
100

654

Figure S5: Percent change [%] between the mean of the monthly river discharge under RCP 8.5 (Figure 5) and the RCP 4.5 scenario (Figure S4).

S1.Climate Indices Toolbox

In this study, we used the Climate Indices Toolbox to calculate the metrics that can characterize the condition of streamflow (e.g., magnitude, frequency and timing; Figure S4 and S5). This toolbox has developed in MATLAB and is able to calculate and compares a suite of more than 250+ metrics for hydroclimate variables among two distinct time span of interests (Table S6 for the list of these metrics). The user can simply use a Graphical User Interface (GUI) or a script to execute the underlying functions and compute the hydroclimate indices of interest by dividing the data into two periods.

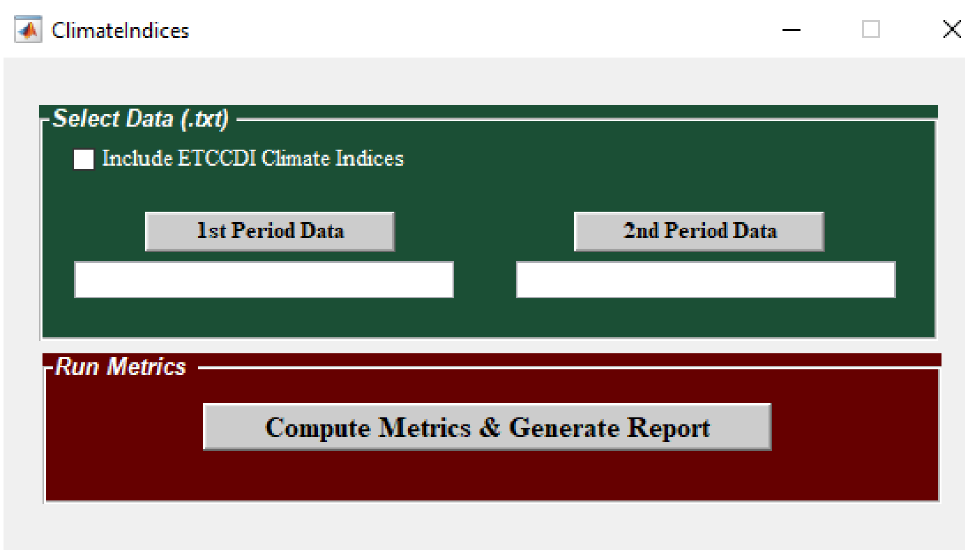

Figure S4. The GUI to execute the Climate Indices Toolbox. If the user select the option of calculating the ETTCDI climate indices, detailed daily information about precipitation, maximum and minimum daily temperature is required. The two buttons "1st and 2nd Period Data" will open browsers for the user to select input data (text file) for each period.

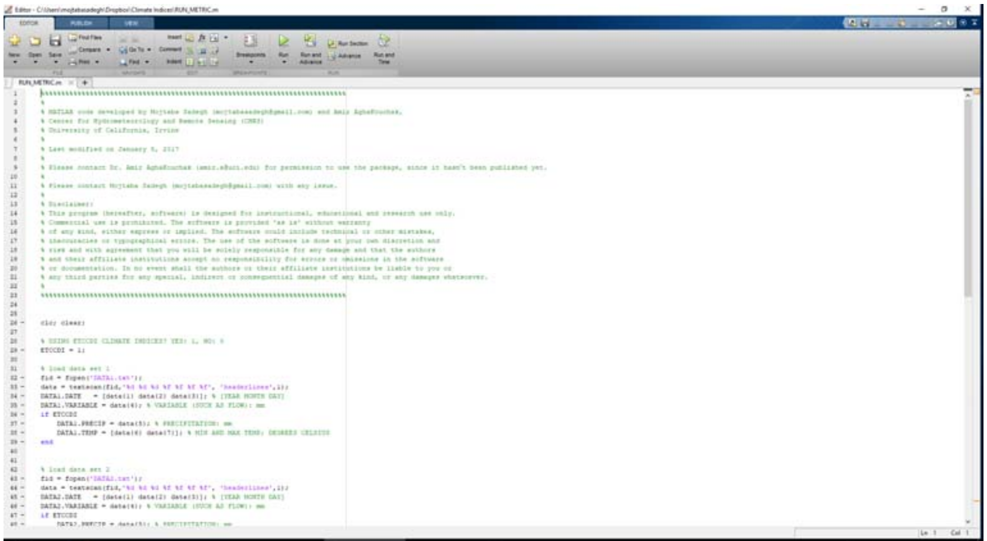

Figure S5. The script file to run the Climate Indices Toolbox. Detailed description is provided in the script to guide the users to select proper option.

Input data to the toolbox should be prepared as the text file with the first line will read as header and at least four and at maximum seven columns. The first three columns identify the year, month and day, respectively. The fourth column in the input data is the hydroclimate variable of interest and might be any hydroclimatological variable such as streamflow, precipitation, temperature, etc. The next three columns are arbitrary and are only to be provided if the user wishes to calculate ETTCDI climate indices that are based on the European Climate Assessment (http://etccdi.pacificclimate.org/list_27_indices.shtml). These three columns take daily values of precipitation, maximum and minimum daily temperature, with a fixed order.

Upon executing the Climate Indices Toolbox, a summary report file (text format) is generated that details the metric values for the first and second selected periods, as well as the change in the magnitude of the metric and percent change between the selected periods. Metrics are ranked in descending order based on absolute value of percent change. Metrics used in the Climate Indices Toolbox are described in Table S6.

Table S6. Description of metrics available in the Climate Indices Toolbox.

Metric Name	Description	Reference
Slope of survival curve	Difference between natural log of 5th and 95th percentiles divided by 0.9 (0.95-0.05)	Ref. 2
Slope of survival curve	Difference between natural log of 33th and 66th percentiles divided by 0.33 (0.66-0.33)	Ref. 3 & 5
Slope of survival curve	Difference between natural log of 20th and 70th percentiles divided by 0.5 (0.70-0.20)	Ref. 9
Volume of high segment in survival curve	Volume (area under survival curve) of variable when it is above 98th percentile	Ref. 9
Volume of low segment in survival curve	Volume of "natural log of variable when it is below 30th percentile minus log of minimum value of the variable"	Ref. 9
Median of survival curve	Median of natural log of variable	Ref. 9 & 10
Autocorrelation of the variable with 1 day lag		Ref. 6
Slope of peak distribution	Difference between 50th and 90th percentiles of peak distribution divided by 0.4 (0.9-0.4). Peaks are higher in value than their neighboring observations.	Ref. 6 & 7
Rising limb density	number of peaks divided by total length of rising limbs	Ref. 6 & 8
Declining limb density	number of peaks divided by total length of declining limbs	Ref. 6 & 8
Variable distribution	1, 5, 15, 50, 95, 99th percentiles	Ref. 13
Mean daily		Ref. 1
Median daily		Ref. 1
Variability	Coefficient of variation in daily variable	Ref. 1
Variability	Coefficient of variation of natural log of {5, 10, ..., 95}th percentiles	Ref. 1
Skewness	Mean daily divided by median daily variable	Ref. 1
Range in daily variable	Ratio of 10th to 90th percentiles	Ref. 1
Range in daily variable	Ratio of 20th to 80th percentiles	Ref. 1

Range in daily variable	Ratio of 25th to 75th percentiles	Ref. 1
Spread in daily variable	Ratio of 10th to 90th percentiles divided by median daily variable	Ref. 1
Spread in daily variable	Ratio of 20th to 80th percentiles divided by median daily variable	Ref. 1
Spread in daily variable	Ratio of 25th to 75th percentiles divided by median daily variable	Ref. 1
Mean monthly variable for …	January, February, March, April, May, June, July, August, September, October, November, December	Ref. 1
Variability in monthly variable for …	Coefficient of variation (standard deviation/mean) for January, February, March, April, May, June, July, August, September, October, November, December	Ref. 1
Variability across monthly variable	Range of monthly flows divided by median monthly variable	Ref. 1
Variability across monthly variable	Interquartile monthly flows divided by median monthly variable	Ref. 1
Variability across monthly variable	Difference between 10th and 90th percentile monthly flows divided by median monthly variable	Ref. 1
Variability across monthly variable	Coefficient of variation in mean monthly variable	Ref. 1
Skewness in monthly variable	"Mean monthly minus median monthly" divided by median monthly variable	Ref. 1
Variability across yearly variable	Range of yearly variable divided by median yearly variable	Ref. 1
Variability across yearly variable	Interquartile of yearly variable divided by median yearly variable	Ref. 1
Variability across yearly variable	Difference between 10th and 90th percentiles yearly variable divided by median yearly variable	Ref. 1

Skewness in annual variable	“Mean annual minus median annual variable” divided by median annual variable	Ref. 1
Mean of monthly min variable across all years for …	January, February, March, April, May, June, July, August, September, October, November, December	Ref. 1
Variability of min monthly variable	Coefficient of variation in min monthly variables	Ref. 1
Mean of annual daily min variable divided by annual median variable, averaged across all years		Ref. 1
Mean of annual min variable divided by mean annual variable, averaged across all years		Ref. 1
Median of annual min variable divided by annual mean variable over all years		Ref. 1
Mean of 7day minimum flow (sum) divided by annual mean variable, averaged across all years		Ref. 1
Coefficient of variation in “7day minimum variable (sum) divided by annual mean variable”		Ref. 1
Mean of “annual min variable divided by annual mean variable” averaged across all years		Ref. 1
Mean of coefficient of variation in monthly min variable, averaged over all years		Ref. 1
Coefficient of variation in annual min variable		Ref. 1

Mean of monthly max variable across all years for …	January, February, March, April, May, June, July, August, September, October, November, December	Ref. 1
Coefficient of variation in “mean monthly max variable”		Ref. 1
Median of “annual max variable divided by annual median variable”		Ref. 1
Mean of annual 99th percentile divided by annual median variable, averaged across all years		Ref. 1
Mean of annual 90th percentile divided by annual median variable, averaged across all years		Ref. 1
Mean of annual 75th percentile divided by annual median variable, averaged across all years		Ref. 1
Coefficient of variation in log of annual max variable		Ref. 1
Skewness in annual max variable	(NYEARS*sum(log(VARIABLE_MAX_PERYEAR.^3)) - 3*NYEARS* sum(log(VARIABLE_MAX_PERYEAR)) *sum(log(VARIABLE_MAX_PERYEAR.^2)) + 2*sum(log(VARIABLE_MAX_PERYEAR)) ^3) / (NYEARS*(NYEARS-1)*(NYEARS-2)*std(VARIABLE_MAX_PERYEAR));	Ref. 1
Mean of annual high variable volume (variable more than annual median) divided by annual median variable, averaged across all years		Ref. 1
Mean of annual high variable volume (variable more than 3*annual median) divided by		Ref. 1

annual median variable, averaged across all years		
Mean of annual high variable volume (variable more than 7*annual median) divided by annual median variable, averaged across all years		Ref. 1
Mean of annual high variable peak (variable more than annual median) divided by annual median variable, averaged across all years		Ref. 1
Mean of annual high variable peak (variable more than 3*annual median) divided by annual median variable, averaged across all years		Ref. 1
Mean of annual high variable peak (variable more than 7*annual median) divided by annual median variable, averaged across all years		Ref. 1
Mean of annual high variable peak (variable more than annual 75th percentile) divided by annual median variable, averaged across all years		Ref. 1
Coefficient of variation in monthly max variable		Ref. 1
Mean “number of annual occurrences during which variable remains below 25th percentile of the variable”, averaged across all years		Ref. 1
Coefficient of variation of “number of annual occurrences during which variable remains		Ref. 1

below 25th percentile of the variable”		
Frequency of low variable spells	Total number of days with low variable (below 0.05*mean of the variable) divided by the number of years of data	Ref. 1
Mean “number of annual occurrences during which variable remains above 75th percentile of the variable”, averaged across all years		Ref. 1
Coefficient of variation of “number of annual occurrences during which variable remains above 75th percentile of the variable”		Ref. 1
Mean “number of annual occurrences during which variable remains above 3*median of the variable”, averaged across all years		Ref. 1
Mean “number of annual occurrences during which variable remains above 7*median of the variable”, averaged across all years		Ref. 1
Mean “number of annual occurrences during which variable remains above median of the variable”, averaged across all years		Ref. 1
Mean “number of annual occurrences during which variable remains above 25th percentile of the variable”, averaged across all years		Ref. 1
Mean “number of annual occurrences during which variable remains above median		Ref. 1

of annual maxima", averaged across all years		
Mean of "annual minima of 1-day mean of daily discharge", averaged across all years		Ref. 1
Mean of "annual minima of 3-day mean of daily discharge", averaged across all years		Ref. 1
Mean of "annual minima of 7-day mean of daily discharge", averaged across all years		Ref. 1
Mean of "annual minima of 30-day mean of daily discharge", averaged across all years		Ref. 1
Mean of "annual minima of 90-day mean of daily discharge", averaged across all years		Ref. 1
Coefficient of variation of "annual minima of 1-day mean of daily discharge"		Ref. 1
Coefficient of variation of "annual minima of 3-day mean of daily discharge"		Ref. 1
Coefficient of variation of "annual minima of 7-day mean of daily discharge"		Ref. 1
Coefficient of variation of "annual minima of 30-day mean of daily discharge"		Ref. 1
Coefficient of variation of "annual minima of 90-day mean of daily discharge"		Ref. 1
Mean of "annual minima of 1-day mean of daily discharge		Ref. 1

divided by median variable", averaged over all years		
Mean of "annual minima of 7-day mean of daily discharge divided by median variable", averaged over all years		Ref. 1
Mean of "annual minima of 30-day mean of daily discharge divided by median variable", averaged over all years		Ref. 1
Mean of "annual mean of variable below 25th percentile divided by annual median variable", averaged across all years		Ref. 1
Mean of "annual mean of variable below 10th percentile divided by annual median variable", averaged across all years		Ref. 1
Low variable pulse duration	Mean "duration of annual occurrences during which variable remains below 25th percentile of the variable", averaged across all years	Ref. 1
Coefficient of variation in "duration of annual occurrences during which variable remains below 25th percentile of the variable"		Ref. 1
Mean annual number of days in which variable has a zero value		Ref. 1
Coefficient of variation of annual number of days in which variable has a zero value		Ref. 1
Percent of months having zero variable		Ref. 1

Mean of “annual maxima of 1-day mean of daily discharge”, averaged across all years		Ref. 1
Mean of “annual maxima of 3-day mean of daily discharge”, averaged across all years		Ref. 1
Mean of “annual maxima of 7-day mean of daily discharge”, averaged across all years		Ref. 1
Mean of “annual maxima of 30-day mean of daily discharge”, averaged across all years		Ref. 1
Mean of “annual maxima of 90-day mean of daily discharge”, averaged across all years		Ref. 1
Coefficient of variation of “annual maxima of 1-day mean of daily discharge”		Ref. 1
Coefficient of variation of “annual maxima of 3-day mean of daily discharge”		Ref. 1
Coefficient of variation of “annual maxima of 7-day mean of daily discharge”		Ref. 1
Coefficient of variation of “annual maxima of 30-day mean of daily discharge”		Ref. 1
Coefficient of variation of “annual maxima of 90-day mean of daily discharge”		Ref. 1
Mean of “annual maxima of 1-day mean of daily discharge divided by median variable”, averaged over all years		Ref. 1

Mean of “annual maxima of 7-day mean of daily discharge divided by median variable”, averaged over all years		Ref. 1
Mean of “annual maxima of 30-day mean of daily discharge divided by median variable”, averaged over all years		Ref. 1
Mean “duration of annual high variable pulses (above 75th percentile of the variable)”		Ref. 1
Coefficient of variation in “duration of annual high variable pulses (above 75th percentile of the variable)”		Ref. 1
Mean “duration of annual high variable pulses (above median of the variable)”		Ref. 1
Mean “duration of annual high variable pulses (above 3*median of the variable)”		Ref. 1
Mean “duration of annual high variable pulses (above 7*median of the variable)”		Ref. 1
Mean “duration of annual high variable pulses (above 25th percentile of the variable)”		Ref. 1
Rise rate	Mean rate of positive changes from one day to the next	Ref. 1
Variability in rise rate	Coefficient of variation in rate of positive changes from one day to the next	Ref. 1
Fall rate	Mean rate of negative changes from one day to the next	Ref. 1
Variability in fall rate	Coefficient of variation in rate of negative changes from one day to the next	Ref. 1

Ratio of days when variable is higher than the previous day		Ref. 1
Median of difference between log of increasing variables		Ref. 1
Median of difference between log of decreasing variables		Ref. 1
Reversals	Number of negative and positive changes from one day to next	Ref. 1
Coefficient of variation in number of negative and positive changes from one day to next		Ref. 1
ETCCDI metrics		
Max Tmax	Max value of daily max temperature for January, February, March, April, May, June, July, August, September, October, November, December	Ref. 14
Max Tmin	Max value of daily min temperature for January, February, March, April, May, June, July, August, September, October, November, December	Ref. 14
Min Tmax	Min value of daily max temperature for January, February, March, April, May, June, July, August, September, October, November, December	Ref. 14
Min Tmin	Min value of daily min temperature for January, February, March, April, May, June, July, August, September, October, November, December	Ref. 14
Cool nights	Percentage of time when daily min temperature is less than 10th percentile	Ref. 14
Cool days	Percentage of time when daily max temperature is less than 10th percentile	Ref. 14

Warm nights	Percentage of time when daily min temperature is more than 90th percentile	Ref. 14
Warm days	Percentage of time when daily max temperature is more than 90th percentile	Ref. 14
Diurnal temperature range	Monthly mean difference between daily max and min temperature for January, February, March, April, May, June, July, August, September, October, November, December	Ref. 14
Growing season length	Annual count between first span of at least 6 days with TG>5 Celsius and first span after July 1 of 6 days with TG<5 Celsius	Ref. 14
Frost days	Annual count when daily min temperature is less than 0 Celsius	Ref. 14
Summer days	Annual count when daily max temperature is more than 25 Celsius	Ref. 14
Tropical nights	Annual count when daily min temperature is more than 20 Celsius	Ref. 14
Warm spell duration indicator	Annual count when at least 6 consecutive days of max temperature is more than 90th percentile	Ref. 14
Cold spell duration indicator	Annual count when at least 6 consecutive days of min temperature is less than 10th percentile	Ref. 14
Max 1-day precipitation amount	Monthly maximum 1-day precipitation for January, February, March, April, May, June, July, August, September, October, November, December	Ref. 14
Max 5-day precipitation amount	Monthly maximum 5-day precipitation for January, February, March, April, May, June, July, August, September, October, November, December	Ref. 14
Simple daily intensity index	The ratio of annual total precipitation to the number of wet days (>= 1 mm)	Ref. 14

Number of heavy precipitation days	Annual count when precipitation >=10 mm	Ref. 14
Number of very heavy precipitation days	Annual count when precipitation >=20 mm	Ref. 14
Consecutive dry days	Maximum number of consecutive days when precipitation <1 mm	Ref. 14
Consecutive wet days	Maximum number of consecutive days when precipitation >=1 mm	Ref. 14
Very wet days	Annual total precipitation from days >95th percentile	Ref. 14
Extremely wet days	Annual total precipitation from days >99th percentile	Ref. 14
Annual total wet-day precipitation	Annual total precipitation from days >= 1 mm	Ref. 14

References:

Ref. 1: Olden, Julian D., and N. L. Poff. "Redundancy and the choice of hydrologic indices for characterizing streamVARIABLE regimes." River Research and Applications 19.2 (2003): 101-121.

Ref. 2: Gustard, Alan, Andrew Bullock, and J. M. Dixon. Low VARIABLE estimation in the United Kingdom. Institute of Hydrology, 1992.

Ref. 3: Carrillo, G., et al. "Catchment classification: hydrological analysis of catchment behavior through process-based modeling along a climate gradient." Hydrology and Earth System Sciences 15.11 (2011): 3411-3430.

Ref. 4: Arnold, Jeffrey G., and P. M. Allen. "Automated methods for estimating baseVARIABLE and ground water recharge from streamVARIABLE records1." (1999): 411-424.

Ref. 5: Yadav, Maitreya, Thorsten Wagener, and Hoshin Gupta. "Regionalization of constraints on expected watershed response behavior for improved predictions in ungauged basins." Advances in Water Resources 30.8 (2007): 1756-1774.

Ref. 6: Euser, Tanja, et al. "A framework to assess the realism of model structures using hydrological signatures." Hydrology and Earth System Sciences, 17 (5), 2013 (2013).

Ref. 7: Sawicz, K., Wagener, T., Sivapalan, M., Troch, P. A., and Carrillo, G.: Catchment classification: empirical analysis of hydrologic similarity based on catchment function in the eastern USA, Hydrol. Earth Syst. Sci., 15, 2895-2911, doi:10.5194/hess-15-2895-2011, 2011.

Ref. 8: Shamir, Eylon, et al. "The role of hydrograph indices in parameter estimation of rainfall–runoff models." Hydrological Processes 19.11 (2005): 2187-2207.

Ref. 9: Mendoza, Pablo A., et al. "Effects of hydrologic model choice and calibration on the portrayal of climate change impacts." Journal of Hydrometeorology 16.2 (2015): 762-780.

Ref. 10: Yilmaz, Koray K., Hoshin V. Gupta, and Thorsten Wagener. "A process?based diagnostic approach to model evaluation: Application to the NWS distributed hydrologic model." Water Resources Research 44.9 (2008).
Ref. 11: Patil, Sopan, and Marc Stieglitz. "Controls on hydrologic similarity: role of nearby gauged catchments for prediction at an ungauged catchment." Hydrology and Earth System Sciences 16.2 (2012): 551-562.
Ref. 12: Sankarasubramanian, A., Richard M. Vogel, and James F. Limbrunner. "Climate elasticity of streamVARIABLE in the United States." Water Resources Research 37.6 (2001): 1771-1781.
Ref. 13: Westerberg, I. K., and H. K. McMillan. "Uncertainty in hydrological signatures." Hydrology and Earth System Sciences 19.9 (2015): 3951-3968.
Ref. 14: Zhang, Xuebin, and Francis W. Zwiers. "Statistical indices for the diagnosing and detecting changes in extremes." Extremes in a Changing Climate. Springer Netherlands, 2013. 1-14.